

Expression and Characterization of the NBD1-R Domain Region of CFTR: Evidence for Subunit–Subunit Interactions[†]

David C. A. Neville, Christine R. Rozanas, Barry M. Tulk, R. Reid Townsend, and A. S. Verkman*

Departments of Medicine and Physiology, Cardiovascular Research Institute, and Department of Pharmaceutical Chemistry, Cystic Fibrosis Research Center, University of California, San Francisco, California 94143-0521

Received August 14, 1997; Revised Manuscript Received November 3, 1997

ABSTRACT: To study interactions between the contiguous NBD1 and R domains of CFTR, wild-type and $\Delta F508$ NBD1-R (amino acids 404–830, in fusion with His₆ tag) were expressed as single proteins in *Escherichia coli*. NBD1-R (10–25 mg/L culture) was purified from inclusion bodies in 8 M urea by Ni-affinity chromatography, and renatured by rapid dilution at pH 5. In vitro phosphorylation by protein kinase A increased the apparent size of NBD1-R from ~52 to ~56 kDa by SDS–PAGE. The fluorescent ATP analogue TNP-ATP bound to renatured NBD1-R with K_d^{app} of $0.81 \pm 0.1 \mu M$ (wild-type), $0.93 \pm 0.1 \mu M$ (wild-type, phosphorylated), $0.75 \pm 0.1 \mu M$ ($\Delta F508$ NBD1-R), and $0.72 \pm 0.1 \mu M$ ($\Delta F508$ NBD1-R, phosphorylated) with a stoichiometry of ~1 TNP-ATP site per NBD1-R molecule; TNP-ATP binding was reversed by ATP, AMP-PCP, and AMP-PNP with K_i s of ~3.2, 4.2, and 4.6 mM, respectively. Secondary structure analysis by circular dichroism gave 19% α -helix, 43% β -sheet and turn, and 38% “other” structure. To determine if nucleotide binding to NBD1 influenced R domain phosphorylation, NBD1-R was in vitro phosphorylated with protein kinase A and [γ -³²P]ATP in the presence of AMP-PCP, AMP-PNP, or TNP-ATP. Whereas the nucleotide analogues did not affect ³²P-incorporation in control proteins (Kemptide, GST-R domain), phosphorylation of NBD1-R was reduced >75% by AMP-PNP or AMP-PCP (0.25 mM) and >50% by TNP-ATP (0.25 μM). Analysis of phosphorylation sites indicated that inhibition involved multiple sites in NBD1-R, including serines 660, 712, 737, 795, and 813. These results establish the conditions for NBD1-R expression, purification, and renaturation. The inhibition of R domain phosphorylation by nucleotide binding to the NBD1 domain indicates significant domain–domain interactions and suggests a novel mechanism for regulation of CFTR phosphorylation.

The cystic fibrosis transmembrane conductance regulator (CFTR)¹ is a 1480 amino acid protein that functions as a plasma membrane chloride channel (1, 2). CFTR is predicted to contain two transmembrane domains and three polar cytoplasmic domains: two nucleotide-binding domains (NBD1 and NBD2) and a highly charged regulatory (R) domain (3). Phosphorylation of one or more of the 10 protein kinase A (PKA) consensus sequences within the R domain activates the CFTR chloride conductance (4, 5).

Binding and hydrolysis of ATP by the NBDs is involved in chloride channel opening and inactivation (6). NBD1 and NBD2 may have distinct functions in controlling channel activity (7); ATP hydrolysis at NBD1 appears to be involved in channel opening whereas ATP binding and hydrolysis by NBD2 results in chloride channel inactivation (8). A recent study reported that the membrane-spanning domains are needed for physical interaction between the two halves of the protein but that the cytoplasmic domains were not required for association under the solubilization and immunoprecipitation conditions used (9). There is little experimental data on the structure or physical disposition of the NBD1, NBD2, or R domains, nor is there information about whether interaction between these domains is important for CFTR function.

Several studies have reported the expression and purification of individual soluble domains of CFTR. An NBD1 fragment has been chemically synthesized (10) and NBD1 has been expressed in bacteria in various fusion constructs (11–14). Recombinant NBD1 binds the fluorescent nucleotide analogue TNP-ATP (12–17) and was shown for one construct to have ATPase activity (18). Comparisons of wild-type and $\Delta F508$ NBD1 suggest that the $\Delta F508$ deletion affects the dynamics of protein folding rather than the final NBD1 conformation (15, 16). The R domain has

[†] Supported by a grant from the Cystic Fibrosis Foundation (CFRDP R613) and NIH Grant HL42368.

* Address correspondence to 1246 Health Sciences East Tower, Cardiovascular Research Institute, University of California, San Francisco, CA 94143-0521. Phone: (415)-476-8530. Fax: (415)-665-3847. E-mail: verkman@itsa.ucsf.edu.

¹ Abbreviations: AMP-PNP, adenylyl-imidodiphosphate; AMP-PCP, adenylyl-(β -, γ -methylene)-diphosphonate; β -ME, β -mercaptoethanol; BSA, bovine serum albumin; CFTR, cystic fibrosis transmembrane conductance regulator; DTT, dithiothreitol; ER, endoplasmic reticulum; GST, glutathione-S-transferase; IPTG, isopropylthio- β -D-galactoside; MBP, maltose binding protein; NBD1-R, recombinant protein consisting of the first nucleotide binding domain (NBD) and the regulatory domain (R) of CFTR (residues 404–830); NTA, nitrilotriacetic acid; MALDI/MS, matrix-assisted laser desorption mass spectrometry; PKA, catalytic subunit of cAMP-dependent protein kinase A; PMSF, phenylmethanesulfonyl fluoride; RP-HPLC, reverse phase HPLC; SDS–PAGE, sodium dodecyl sulfate–polyacrylamide gel electrophoresis; TCA, trichloroacetic acid; TFA, trifluoroacetic acid; TNP-ATP, 2'-(or 3')-O-(trinitrophenyl)-adenosine triphosphate.

also been expressed in bacteria (19–22) for determination of *in vitro* sites of phosphorylation by PKA, and in Sf9 cells (23, 24) for studies of interactions with a coexpressed NBD1 construct. Recently, bacterial expression of NBD1-R as a single His₆-tagged protein (amino acids 348–827, 438–827) was attempted (25); however, the expression level was too low (<1.5 mg/L bacterial culture) to permit assay of nucleotide binding or secondary structure.

The objective of this study was to express, purify, and renature wild-type and Δ F508 NBD1-R domain proteins for analysis of nucleotide binding, phosphorylation, and secondary structure. Expression of the NBD1 and R domains as a single fusion protein also permitted the direct examination of putative domain–domain interactions, including effects of R domain phosphorylation on nucleotide binding and effects of nucleotide binding to NBD1 on R domain phosphorylation. A secondary motivation for expression of the NBD1 and R domains together was for crystallization trials in which preservation of native domain–domain interactions may be important. The NBD1-R protein was expressed in *E. coli*, purified from inclusion bodies under denaturing conditions, and renatured by a rapid dilution procedure. The wild-type and Δ F508 NBD1-R proteins were characterized in terms of nucleotide binding, secondary structure and phosphorylation, and significant domain–domain interactions were found.

MATERIALS AND METHODS

Chemicals. Chemicals were obtained from Sigma (St. Louis, MO) unless otherwise specified. ATP, AMP-PCP, AMP-PNP, BSA, and DNase I were purchased from Boehringer Mannheim (Indianapolis, IN), [γ -³²P]-ATP (6000 Ci/mmol) from Amersham Life Science (Arlington Heights, IL), cAMP-dependent protein kinase (catalytic subunit) and sequencing grade trypsin from Promega (Madison, WI), TNP-ATP from Molecular Probes (Eugene, OR), IPTG from Gibco BRL (Gaithersburg, MD), and Ni-NTA agarose from Qiagen (Chatsworth, CA).

Expression of NBD1-R, Δ F508 NBD1-R and GST-R Proteins. Expression of NBD1-R was performed essentially as described (26). For Δ F508 NBD1-R, full-length human Δ F508 CFTR cDNA was used as a template for amplification of bp 1342–2619 corresponding to amino acids 404–829 (exons 9–13) of Δ F508 NBD1-R. Transformed *Escherichia coli* was used to inoculate either LB or NZCYM medium (containing 50 μ g/mL or 100 μ g/mL ampicillin, respectively), which was grown for 1 h at 37 °C and induced with 1 mM IPTG for 2 h. Bacteria were recovered by centrifugation at 7000g, resuspended in Laemmli sample buffer, and analyzed by 12% SDS–PAGE. Cultures expressing recombinant NBD1-R protein at high levels were chosen for large scale purification.

Control experiments were done using the recombinant R domain peptide (exon 13, amino acids 589–830) in fusion with glutathione-S-transferase (GST-R, 54 kDa). DNA encoding the R domain was subcloned into plasmid pGEX (Pharmacia) which contained an in-frame upstream GST cDNA. *E. coli* JM109 expressing GST-R protein were lysed as described below, the cell pellet was washed with Triton X-100, and inclusion bodies were solubilized in 0.1 M NaH₂PO₄, 8 M urea (pH 8).

Purification of NBD1-R. Recombinant protein was generally purified from 1.5 L cultures of *E. coli* transformed with pRSETA-NBD1-R or pRSETA- Δ F508-NBD1-R. A 150 mL culture grown overnight was used to inoculate 1350 mL of medium (LB or NZCYM) containing ampicillin. The bacteria were grown to an optical density of 0.6–0.8 OD units at 600 nm (~1.5 h) and then induced for 2–3 h by addition of 1 mM IPTG. Cells were recovered by centrifugation at 7000g and stored frozen at –20 °C. The cell pellets were lysed by lysozyme (0.5 mg/mL) in 150 mL Tris buffer (10 mM Tris-HCl, pH 8, 1 mM EDTA) at 4 °C for 30 min. After addition of MgSO₄ (10 mM) and DNase I (10 units) and incubation for an additional 30 min, the solution was sonicated and centrifuged at 7000g for 20 min at 4 °C. The pellet, which contained recombinant proteins in inclusion bodies, was resuspended in 50 mL of 10 mM Tris buffer containing 1% Triton X-100, incubated for 10 min on ice, and centrifuged at 10000g for 20 min at 4 °C.

Metal-ion affinity chromatography was used to isolate the His₆-tagged proteins. Inclusion bodies were solubilized in 0.1 M NaH₂PO₄ (pH 8), 8 M urea (buffer A) containing 10 mM β -ME and briefly centrifuged to remove insoluble material. The supernatant was applied to a 2 mL gravity-flow column containing Ni²⁺-nitrilotriacetic acid (Ni-NTA) agarose equilibrated in buffer A. The column was washed with 5 column volumes of buffer A containing 10 mM β -ME and then with buffer A containing 10 mM β -ME at pH 6.3 until eluant absorbance at 280 nm was near zero (~5 column volumes). The bound protein was eluted in 1 mL fractions with 5 column volumes of buffer A at pH 4.5. NBD1-R protein yield was 10–25 mg/L of bacterial culture.

Several procedures were used to remove minor contaminants in some experiments (see Results). Inclusion bodies were suspended in 10 mM Tris (pH 8) and 10 mM β -ME and purified by centrifugation through a 50% sucrose cushion for 30 min at 15000g. In some studies, inclusion bodies were incubated in 1% octylglucoside, 10 mM Tris-HCl, and 1 mM EDTA (pH 8) at 37 °C for 16 h prior to solubilization. Low molecular weight contaminants were removed using size exclusion chromatography (TSK-3000, TosoHaas, Montgomeryville, PA), eluting in 0.1 M Tris (pH 7.4), 8 M urea, and 10 mM DTT. Alternatively, 1–2 mg of the Ni-NTA-purified recombinant protein was injected onto analytical scale C₄, C₈, and C₁₈ reverse phase columns equilibrated in 2% acetonitrile, and 0.1% aqueous TFA. Columns were eluted with a linear gradient of 2–70% acetonitrile at 1 mL/min, followed by a wash with 98% acetonitrile, 0.08% TFA.

Renaturation of NBD1-R. Several methods were investigated to reduce denaturant concentration. Method 1: *column renaturation.* Ni-NTA-purified NBD1-R (10 mg) was reapplied to an Ni-NTA column equilibrated in 6 M urea, 0.5 M NaCl, 20% glycerol, and 20 mM Tris (pH 8) at a flow rate of 1 mL/min. The concentration of urea was reduced by washing the column with a linear gradient of 6:1 M urea in 0.5 M NaCl, 20% glycerol, and 20 mM Tris (pH 8) over 90 min at 1 mL/min. Soluble protein was eluted with 250 mM imidazole. Method 2: *slow dialysis.* NBD1-R was diluted to 50 μ g/mL with buffer A containing PMSF (1 mM), leupeptin (100 μ M), and pepstatin (1 mM) and dialyzed at 4 °C for 12 h against 200 vol of 4 M urea, 50 mM Tris (pH 8.5), 150 mM NaCl, and 2 mM DTT. The protein was then dialyzed against 2 M urea, 50 mM Tris (pH 8.5), 150

mM NaCl, and 2 mM DTT. Final buffer concentrations were reduced to 50 mM Tris (pH 8.5), 125 mM urea, and 10 mM NaCl by serial 2-fold dilutions of the dialysis buffer with 50 mM Tris, pH 8.5 at 12 h intervals. Method 3: *rapid dilution*. The NBD1-R protein concentration was adjusted to ~0.5–1 mg/mL at pH 5 (using acetic acid) and diluted 10–20-fold into 5 mM sodium acetate (pH 5) at 4 or 23 °C. Similarly, the protein solution was adjusted to pH 8 (using NaOH) and diluted 10-fold into 5 mM Tris-HCl (pH 8) with or without the following additives: 0.1% Triton X-100, 10% glycerol, 10 mM DTT, 150 mM NaCl, 0.5 M NaCl, 10 mM MgATP, or 0.1 M L-arginine. Diluted samples were incubated at 4, 23, or 37 °C for 12 h. Samples were centrifuged at 4 °C for 1 h at 100000g to remove insoluble material. The supernatants were assayed for protein concentration using the Bio-Rad protein assay system (Bio-Rad, Hercules, CA) and nucleotide binding (see below).

In vitro Phosphorylation of NBD1-R. Purified NBD1-R (wild-type or $\Delta F508$) (5–50 μ g) in 8 M urea, 0.1 M NaH_2PO_4 was diluted 4-fold into 50 mM Tris-HCl (pH 7.4) and incubated for 2 h at 37 °C in 2 mM MgSO_4 , 1 mM ATP, and 1000 units/mL PKA. Control reactions were performed in the absence of ATP or PKA. Reactions were quenched by addition of 10% TCA (v/v) to precipitate the proteins or 5 \times Laemmli buffer for analysis by 12% SDS-PAGE. In some experiments, NBD1-R (25–50 μ g/mL) was phosphorylated at pH 5 and 23 °C after rapid dilution (see above). To generate partially phosphorylated protein, reactions were performed using 0.1 mM ATP for 30 min at 23 °C.

^{32}P -Labeling of NBD1-R and GST-R. To quantify incorporated phosphate, duplicate samples of the renatured NBD1-R protein (25–40 μ g/mL) were phosphorylated using [γ - ^{32}P]ATP (~0.5 μCi /0.5 mL reaction volume), 0.1 mM ATP, 2 mM MgSO_4 , and 500 units/mL PKA. In some experiments, the protein was preincubated for 15 min prior to addition of the ATP/[γ - ^{32}P]ATP with one of the following: 0.125 or 0.25 mM AMP-PNP, 0.125 or 0.25 mM AMP-PCP, or 0.25 μ M TNP-ATP. GST-R samples (diluted from 8 M urea stock into 5 mM sodium acetate at pH 5 just prior to use) were treated identically. Controls for NBD1-R and GST-R consisted of all reaction components except for PKA. After 30 min at 23 °C, the reactions were quenched with 5 \times Laemmli buffer and analyzed by 12% SDS-PAGE. The gels were stained with Coomassie Blue, destained, dried, and visualized by autoradiography. Band intensities were normalized to protein/lane determined by Coomassie staining.

Phosphorylation of Kemptide. Kemptide (250 μ M) was phosphorylated with 0.1 mM ATP, 2 mM MgSO_4 , 0.8 M urea, 5 mM sodium acetate, and 10 mM NaH_2PO_4 , pH 5.6 for 30 min by adjusting the amount of PKA (generally ~1200 units/mL). These phosphorylation conditions were chosen to give partial phosphorylation (5–6%) in 30 min when analyzed by HPLC on a C_{18} column (determined by area percent at 210 nm absorbance). Phosphorylation of Kemptide was confirmed by MALDI/MS. Kemptide was then phosphorylated in the presence of AMP-PCP, AMP-PNP, or TNP-ATP under identical conditions as described above for NBD1-R and GST-R, and the amount of phosphorylated Kemptide was determined by HPLC.

HPLC Analysis of Phosphopeptides. After phosphorylation of NBD1-R and GST-R as described above, sequencing grade trypsin (1:20 w/w) was added for 2 h. Reactions were

stopped by addition of 5% acetonitrile/0.5% trifluoroacetic acid in water. The reaction mixtures were desalted by RP-HPLC using a 1 \times 150 mm C_{18} column at a flow rate of 50 $\mu\text{L}/\text{min}$ equilibrated with 2% acetonitrile/0.1% trifluoroacetic acid in water. The column eluate was monitored by absorbance at 210 nm. Peptides were collected following stepwise elution to 60% acetonitrile/0.1% trifluoroacetic acid in water. Phosphopeptides were purified by immobilized metal-ion affinity chromatography using iron-loaded NTA agarose and C_{18} RP-HPLC as described (27). Phosphopeptides were identified by comparison with known elution positions of NBD1-R phosphopeptides following C_{18} RP-HPLC (26, 27).

Fluorescent Nucleotide Binding. Nucleotide binding was measured from the fluorescence enhancement of the fluorescent ATP analogue TNP-ATP. Fluorescence was measured on a model 8000c fluorimeter (SLM Instruments, Urbana, IL) at excitation and emission wavelengths of 410 and 540 nm (1 nm slit widths), respectively. Renatured protein (0.02–0.1 mg/mL in 5 mM sodium acetate, pH 5, with 0.4–0.8 M urea, 5–10 mM NaH_2PO_4 , and 2 mM MgSO_4) was incubated with TNP-ATP (0–4.3 μM) by addition of 2–8 μL aliquots of stock 100 μM TNP-ATP solutions (in 5 mM sodium acetate, pH 5, with 0.4–0.8 M urea and 5–10 mM NaH_2PO_4) to a cuvette with continuous stirring. The apparent TNP-ATP dissociation constant (K_d^{app}) was determined by nonlinear least squares regression to the equation $F_c = F_o + F_1\{[\text{TNP-ATP}]/([\text{TNP-ATP}] + K_d^{\text{app}})\}$, where F_o is fluorescence at 0 μM TNP-ATP, F_1 is related to TNP-ATP fluorescence when bound, and F_c is the measured fluorescence corrected for dilution and inner filter effect.

To estimate TNP-ATP site stoichiometry and absolute binding affinity ($K_d = [\text{TNP-ATP}][\text{S}]/[\text{T-S}]$, where $[\text{S}]$ is the concentration of unbound TNP-ATP binding sites on NBD1-R and $[\text{T-S}]$ the concentration of bound TNP-ATP sites), K_d^{app} (from fluorescence vs total $[\text{TNP-ATP}]$ titrations) was measured as a function of NBD1-R concentration. The K_d relation can be rewritten as $K_d = (T_t - [\text{T-S}])(S_t - [\text{T-S}])/[\text{T-S}]$, where T_t is the total added TNP-ATP concentration and S_t total binding site concentration. When 50% of sites are bound ($[\text{T-S}] = S_t/2$), $T_t \approx K_d^{\text{app}}$, so that $K_d^{\text{app}} = K_d + S_t/2$. A linear plot of K_d^{app} vs NBD1 concentration then gives K_d and S_t from the intercept and slope, respectively.

For measurement of TNP-ATP binding reversal, renatured NBD1-R (1 mL, 33 $\mu\text{g}/\text{mL}$) was incubated with TNP-ATP (0–0.4 μM) by addition of 1 μL aliquots of stock 100 μM TNP-ATP solutions (in 5 mM sodium acetate, pH 5, 0.4 M urea, and 5 mM NaH_2PO_4) to a cuvette with continuous stirring. Aliquots (1–4 μL) of stock 0.5 M ATP, AMP-PCP, or AMP-PNP solutions (in 5 mM sodium acetate, pH 5, 0.4 M urea, 5 mM NaH_2PO_4) to 16 mM were added, and fluorescence was measured. K_I for reversal of fluorescent enhancement was calculated using the equation $K_I^{\text{app}} = K_I(1 + [\text{TNP-ATP}]/K_d^{\text{app}})$, where K_I^{app} is the measured concentration of nucleotide that reduced the measured fluorescence enhancement at 0.4 μM TNP-ATP by 50%.

For measurement of TNP-ATP binding after in vitro phosphorylation, renatured NBD1-R (33 $\mu\text{g}/\text{mL}$) and $\Delta F508$ NBD1-R (45 $\mu\text{g}/\text{mL}$) were phosphorylated in the presence

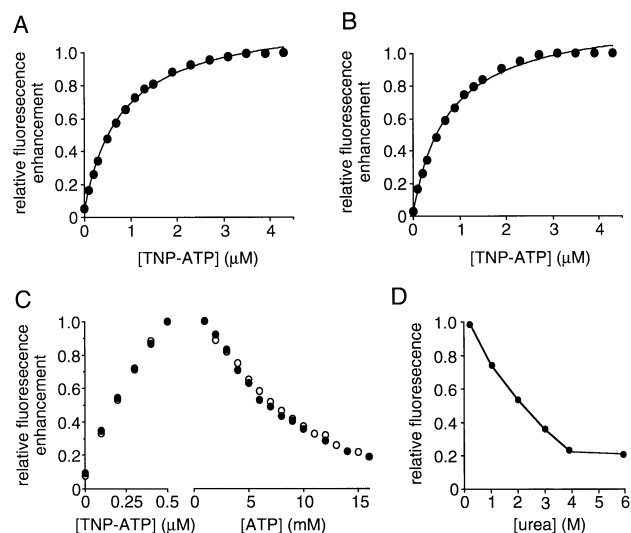


FIGURE 1: Binding of the fluorescent nucleotide TNP-ATP to the NBD1-R and Δ F508 NBD1-R domain proteins. (A) Refolded wild-type NBD1-R (33 μ g/mL) was titrated with TNP-ATP and the fluorescence enhancement was measured ($\lambda_{\text{ex}} = 410$ nm, $\lambda_{\text{em}} = 540$ nm). Measured fluorescence was corrected for background. The fitted curve is shown. See text for fitted K_d values. (B) Titration curves for Δ F508 NBD1-R (45 μ g/mL). (C) Refolded wild-type NBD1-R was titrated with TNP-ATP to approximately half-maximal fluorescence enhancement. Addition of ATP (○, ●), reversed the fluorescence enhancement. See text for fitted K_d values. (D) Refolded NBD1-R (25 μ g/mL) samples were incubated in the indicated urea concentrations for 2 h at 23 °C prior to measurement of maximum TNP-ATP fluorescence enhancement.

of 2 mM MgSO_4 , 500 μ M ATP, and 250 units/mL PKA at 23 °C, pH 5.0, for 60–120 min. The presence of 500 μ M ATP did not interfere with TNP-ATP binding.

Circular Dichroism. CD spectra were measured using a Jasco J-500 spectropolarimeter (Jasco, Tokyo). Sample consisted of NBD1-R (~1 mg/mL in buffer A after Ni-NTA purification) diluted 20-fold into 5 mM sodium acetate at 4 °C, centrifuged at 100000g for 1 h at 4 °C, and concentrated 5–10-fold using Microcon 10 tubes (Amicon, Beverly, MA). CD spectra were measured in 1 mm path length quartz CD cuvettes. Ten scans, at a rate of 50 nm/min, were recorded per measurement. Absorbance was measured on each sample between 190 and 300 nm to rule out aggregation. Temperature melt studies were performed by monitoring molar ellipticity at 222 nm over the temperature range 25–80 °C at a rate of 1 °C/min. Protein secondary structure was determined from CD spectra by numerical decomposition using the basis spectra set of Chang et al. (28).

RESULTS

The NBD1-R and Δ F508 NBD1-R fusion proteins were expressed and purified from *E. coli*. The majority of the fusion protein was present in the insoluble inclusion body fraction as shown previously (26). Expression levels were found empirically to be increased using NZCYM medium in place of LB medium and by incubation at reduced temperatures (30–35 °C) after addition of IPTG.

Wild-type and Δ F508 NBD1-R were purified by Ni-NTA affinity chromatography as described in Materials and Methods. The purified wild-type (see Figure 2A, lanes 1 and 2) and Δ F508 NBD1-R (data not shown) proteins were observed as a single band with predicted $M_r \approx 52$ kDa

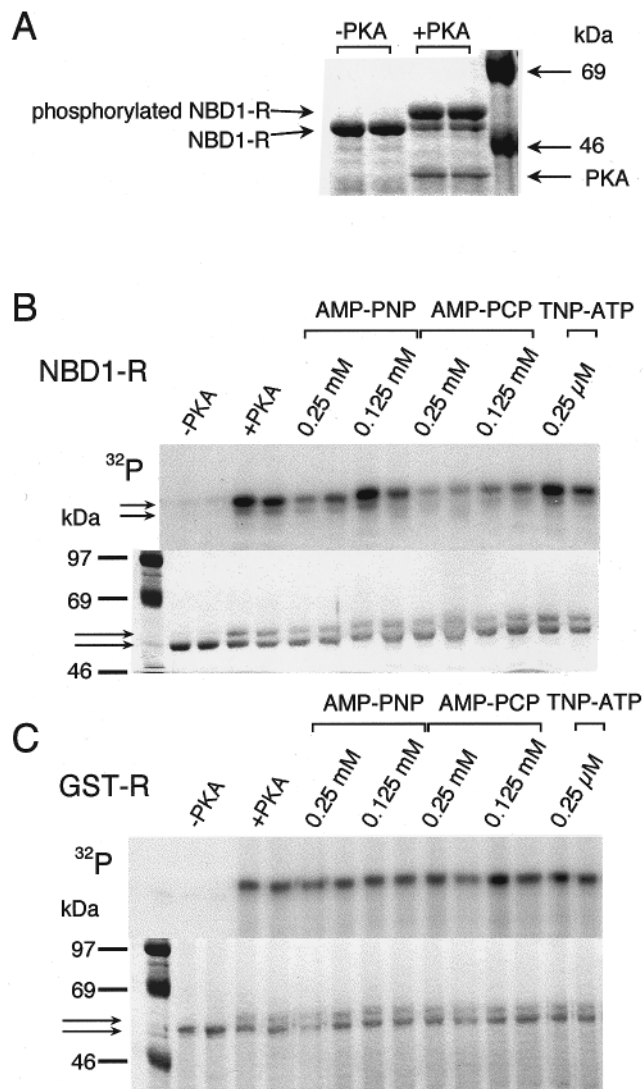


FIGURE 2: Measurement of NBD1-R and GST-R phosphorylation by ^{32}P incorporation. (A) Duplicate samples of wild-type NBD1-R (40 μ g/mL) were phosphorylated with PKA as described in the Materials and Methods. Controls reactions were performed in the absence of PKA. 12% SDS-PAGE with Coomassie Blue staining is shown. (B) Duplicate samples of refolded wild-type NBD1-R (40 μ g/mL) were phosphorylated in the presence of $[\gamma\text{-}^{32}\text{P}]\text{-ATP}$ in the absence and presence of AMP-PNP, AMP-PCP or TNP-ATP at the indicated concentrations. Autoradiogram (top) and 12% SDS-PAGE with Coomassie Blue staining (bottom) are shown. (C) GST-R was phosphorylated under identical conditions to NBD1-R and analyzed by 12% SDS-PAGE.

following SDS-PAGE. The yield of purified protein was generally 10–25 mg/L of culture. In some preparations, up to 50% of the bound protein did not elute from the Ni-NTA column at pH 4.5 fraction due to aggregation. This bound protein could be recovered by elution with 6 M guanidine-0.1 M acetic acid, desalting, and reapplication to the column. This material was not used for the experiments performed in this study. In some preparations, lower yields of NBD1-R were found and correlated with the presence of small protein fragments that bound to the Ni-NTA agarose. Although inclusion of protease inhibitors (leupeptin, pepstatin, and PMSF) during cell lysis did not reduce the amount of these contaminants, proteolysis could be reduced by use of a bacterial strain BL21 that is deficient in proteases lon and ompT (Novagen). Two other approaches that were tried for

Table 1: Evaluation of NBD1-R Renaturation by Rapid Dilution^a

pH	temp (°C)	additive	solubility	TNP-ATP binding
5	4	none	+++	yes
5	23	none	+++	yes
5	23	0.1% Triton X-100	+++	yes
8	4	none	++	no
8	23	none	+	no
8	23	0.1% Triton X-100	+++	yes
8	23	10% glycerol	—	ND
8	23	10 mM DTT	++	no
8	23	150 mM NaCl	+++	no
8	23	500 mM NaCl	+++	no
8	23	10 mM MgATP	—	ND
8	23	100 mM L-Arg	+	ND
8	37	none	++	no

^a Ni-NTA-purified NBD1-R was adjusted to either pH 8.0 (NaOH) or pH 5.0 (acetic acid) at 0.5–1 mg/mL protein concentration in 8 M urea. Samples were diluted 10:1 into either 5 mM Tris-HCl (pH 8.0) or 5 mM sodium acetate (pH 5.0) with indicated additives, incubated for 12 h at the indicated temperature and centrifuged at 100000g, 4 °C for 1 h. Solubility was determined by assay of the supernatant protein concentration. TNP-ATP binding was determined by fluorescence titrations. ND, not determined.

purification of NBD1-R after Ni-NTA chromatography were unsuccessful. Size exclusion chromatography under denaturing conditions removed contaminating proteins, but the purified NBD1-R protein could not be refolded efficiently. Attempted purification of NBD1-R by HPLC (C₄, C₈, or C₁₈ analytical columns) did not yield pure protein; the majority of NBD1-R eluted in the 95% acetonitrile column wash, suggesting protein aggregation during adsorption and/or elution.

Rapid dilution, column renaturation, and dialysis were evaluated to refold the NBD1-R protein. Table 1 summarizes a series of conditions tested for reduction of denaturant concentration using rapid dilution. Refolding efficiency was assessed by protein solubility and fluorescent nucleotide binding (see below). Efficient renaturation was found by rapid dilution of the purified NBD1-R at pH 5 and 4 °C. Other conditions known to facilitate protein renaturation were examined (29–33), but were unsuccessful. Addition of Triton X-100 facilitated refolding of NBD1-R at pH 5 or 8, but caused nonspecific TNP-ATP binding and was difficult to remove. For subsequent studies, NBD1-R (0.5–1 mg/mL) in 8 M urea was diluted to give a final buffer composition of 5 mM sodium acetate, 5–10 mM NaH₂PO₄, and 0.4–0.8 M urea. Generally, >80% of the soluble protein was recovered after ultracentrifugation (100000g, 1 h, 4 °C). The diluted protein could be stored at 4 °C for more than 6 months without loss of solubility or nucleotide binding affinity. Attempts to further dialyze the protein to 0 M urea or to concentrate the protein to >100 µg/mL resulted in >50% loss of soluble protein. Reduction of denaturant concentration by step dialysis or column chromatography did not give usable amounts of renatured NBD1-R. In the dialysis method, urea was gradually removed over several days. Under the conditions tested, NBD1-R (initially >25 µg/mL) precipitated at urea concentrations between 2 and 1 M. Reduction of denaturant concentration in situ on the Ni-NTA column, using various step sizes, generally gave <30% recovery of soluble NBD1-R protein.

The fluorescent nucleotide TNP-ATP bound to refolded NBD1-R and ΔF508 NBD1-R with high affinity. Addition

of submicromolar concentrations of TNP-ATP to the renatured proteins produced a significant enhancement in TNP-ATP fluorescence at 540 nm (NBD1-R, Figure 1A; ΔF508 NBD1-R, Figure 1B). Subsequent addition of millimolar concentrations of ATP (Figure 1C), AMP-PCP, and AMP-PNP (not shown) to NBD1-R reversed the fluorescence enhancement. Fitted K_d^{app} for TNP-ATP binding to wild-type NBD1-R was $0.81 \pm 0.1 \mu\text{M}$ and to ΔF508 NBD1-R was $0.75 \pm 0.1 \mu\text{M}$. These results indicate that the ΔF508 deletion has little effect on ATP binding. The K_i values for reversal of the fluorescence enhancement by ATP, AMP-PCP, and AMP-PNP were ~3.2, 4.2, and 4.6 mM, respectively. The molar stoichiometry of TNP-ATP binding to NBD1-R was determined from the dependence of K_d^{app} on NBD1-R concentration as explained in the Materials and Methods. At NBD1-R concentrations of 20, 40, and 60 µg/mL (equivalent to 0.38, 0.77, and 1.15 µM), K_d^{app} values were 0.41, 0.63, and 0.83 µM. The computed molar stoichiometry (bound TNP-ATP to NBD1-R) was 1.09 ± 0.1 , suggesting ~1 TNP-ATP binding site per molecule of renatured NBD1-R. NBD1-R protein folding was sensitive to the urea concentration, losing half of its capacity to bind TNP-ATP at 2 M urea (Figure 1D). These results indicate that nucleotide binding to NBD1-R is specific, reversible, and requires folded protein. The 1:1 stoichiometry and single binding affinity suggest a homogeneous population of NBD1-R; however, heterogeneous subpopulations with similar TNP-ATP binding properties cannot be discounted.

The next set of experiments was designed to determine whether nucleotide binding to NBD1-R affects PKA-mediated phosphorylation. Following SDS-PAGE and Coomassie Blue staining, in vitro phosphorylation by PKA produced a band of higher apparent molecular size (Figure 2A). The reaction was nearly complete in 2–3 h at 1 mM ATP and 23 °C. Similar band appearances were found for phosphorylation of the refolded NBD1-R (in 0.8 M urea at pH 5) vs a 4-fold dilution of the Ni-purified NBD1-R in 2 M urea at pH 7.4 (data not shown). The upper band suggests phosphorylation at ⁷³⁷Ser (34); other sites (nine serines in dibasic consensus sites for PKA-mediated phosphorylation) may also be phosphorylated in the upper band. The minor band that comigrates with the nonphosphorylated protein suggests lack of ⁷³⁷Ser phosphorylation in a subset of the phosphorylated protein.

To quantify NBD1-R phosphorylation, PKA-mediated incorporation of ³²P (from [γ -³²P]ATP) was measured by densitometry of autoradiograms. Phosphorylation reactions were carried out under conditions that gave partial phosphorylation so that increases and decreases could be observed. The majority of ³²P incorporation was found in the upper band (Figure 2B, upper panel), consistent with the conclusion that ⁷³⁷Ser is one of the first sites on the R domain to be phosphorylated by PKA (34). Under the conditions of the assay, the phosphorylation of NBD1-R did not go to completion in either the presence or absence of ATP analogues (Figure 2B, lower panel). Inclusion of the ATP analogues AMP-PNP, AMP-PCP, or TNP-ATP at the time of phosphorylation significantly reduced the incorporation of ³²P (Figure 2B, upper panel).

The inhibition of NBD1-R phosphorylation by nucleotides could be due to competition of nucleotides with ATP, direct

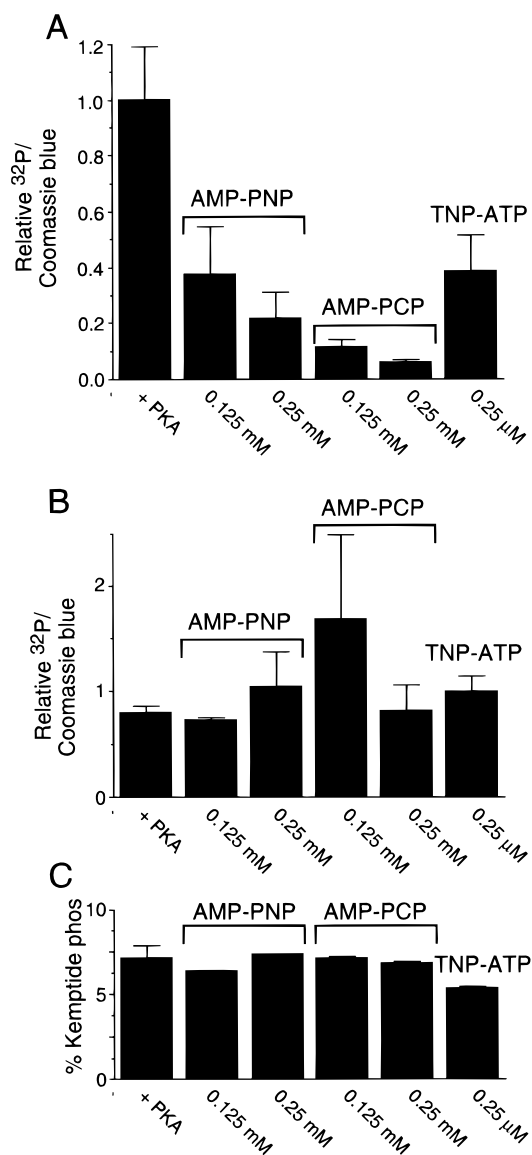


FIGURE 3: Quantitative analysis of the phosphorylation of NBD1-R, GST-R, and Kemptide. (A) NBD1-R. The relative amount of PKA-mediated ^{32}P incorporation normalized to Coomassie Blue stained protein was calculated after densitometry of the autoradiogram/stained gel in Figure 2B. (B) GST-R. Analysis was performed as described for panel A using the autoradiogram/stained gel in Figure 2C. (C) Kemptide. Kemptide was phosphorylated in the absence and presence of AMP-PNP, AMP-PCP, or TNP-ATP. The reaction products were separated by C_{18} RP-HPLC. The column eluant was monitored by measurement of absorbance at 210 nm and the peak areas of the phosphorylated and nonphosphorylated Kemptide calculated.

interaction of nucleotides with PKA or the R domain, and/or binding of nucleotides to the NBD1 domain that then alters the phosphorylation efficiency of the R domain. To distinguish among these possibilities, phosphorylation reactions under identical conditions were done using as substrates (in place of NBD1-R) a GST-R domain fusion protein, or Kemptide (an artificial 7 amino acid peptide with a single PKA consensus site). When AMP-PCP, AMP-PNP, or TNP-ATP were present under conditions in which ^{32}P incorporation into NBD1-R was remarkably decreased (Figure 2B and Figure 3A), no significant differences in the phosphorylation of GST-R (Figure 2C and Figure 3B) or Kemptide (Figure 3C) were observed. These results suggest

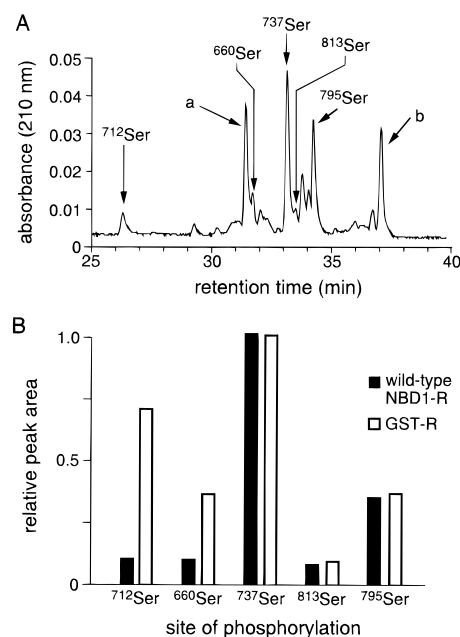


FIGURE 4: Phosphopeptide map of in vitro phosphorylated NBD1-R and GST-R proteins. (A) C_{18} RP-HPLC chromatogram of IMAC purified NBD1-R phosphopeptides. The column eluant was monitored by absorbance at 210 nm. Phosphopeptides were identified from known elution positions as described (26). Peaks marked a and b arise from acidic NBD1-R peptides copurified using IMAC. (B) Relative peak areas of the five principal phosphopeptides in NBD1-R and GST-R. The peak areas for the five phosphopeptides from PKA phosphorylated NBD1-R and GST-R were measured following C_{18} RP-HPLC and normalized to unity for the ^{737}Ser -containing phosphopeptide.

that the inhibition of NBD1-R phosphorylation by nucleotides involves a nucleotide–NBD1 domain interaction that then influences the efficiency of R domain phosphorylation.

To determine whether the pattern of phosphorylated sites was grossly changed upon in vitro phosphorylation of NBD1-R vs GST-R, and without vs with nucleotides, phosphorylated sites were resolved by trypsin digestion, RP-HPLC, and immobilized metal-ion affinity chromatography (see Materials and Methods). Figure 4A shows an RP-HPLC peptide map for PKA phosphorylated NBD1-R. The RP-HPLC peptide map for PKA-phosphorylated GST-R and NBD1-R, and GST-R phosphorylated in the presence of nucleotides were similar (data not shown). In all cases, five major phosphoserine-containing peptides (serines 660, 712, 737, 795, and 813) were observed by this procedure based on previous identifications by mass spectrometry (26). In addition, at least two peaks from acid phosphopeptides (copurified by metal-ion affinity chromatography) were observed. Figure 4B shows relative peak areas of the five principal phosphopeptides from PKA phosphorylated NBD1-R and GST-R. There were quantitative differences in the phosphorylation pattern for ^{712}Ser and ^{660}Ser , probably arising from influences of the NBD1 domain on R domain conformation. These results indicate that multiple sites in the R domain are phosphorylated under the experimental conditions here and that the pattern of phosphorylation is not grossly affected by nucleotides.

Given the effect of nucleotide binding to NBD1 on R domain phosphorylation, the hypothesis was tested that R domain phosphorylation affects nucleotide binding. Wild-

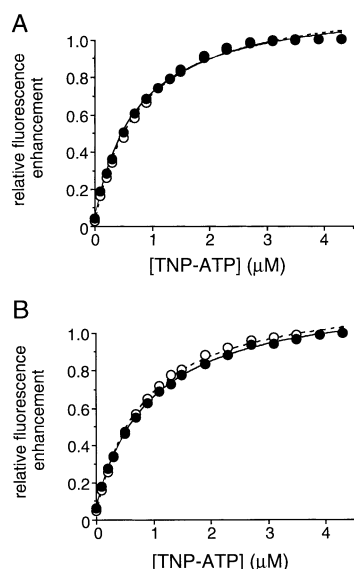


FIGURE 5: Nucleotide binding to phosphorylated NBD1-R and Δ F508 NBD1-R. Wild-type (A) (33 μ g/mL) and Δ F508 NBD1-R (B) (45 μ g/mL) were phosphorylated using PKA (●, —). Control protein (○, ---) was treated identically minus PKA. TNP-ATP fluorescence enhancement was measured as in Figure 1. See text for fitted K_d values.

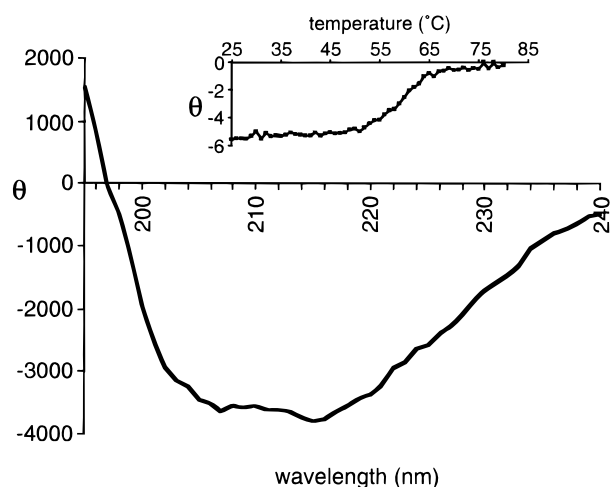


FIGURE 6: Circular dichroism analysis of NBD1-R. Refolded wild-type NBD1-R was analyzed by CD spectroscopy. θ is the measured molar ellipticity. (inset) θ (shown as $\theta/1000$) was continuously monitored at 222 nm while increasing the temperature by 1 $^{\circ}$ C/min.

type NBD1-R and Δ F508 NBD1-R proteins were phosphorylated by PKA and ATP. TNP-ATP fluorescence enhancement data were qualitatively similar for phosphorylated and control NBD1-R (Figure 5A) and Δ F508 NBD1-R (Figure 5B). Fitted K_d^{app} for TNP-ATP binding to PKA phosphorylated wild-type NBD1-R was $0.93 \pm 0.1 \mu\text{M}$ and to PKA-phosphorylated Δ F508 NBD1-R was $0.72 \pm 0.1 \mu\text{M}$. The control sample was generated under the same conditions as the phosphorylated sample except that PKA was not added.

Circular dichroism was done to determine NBD1-R secondary structure. In this experiment, urea was removed from NBD1-R solutions by dialysis against 5 mM sodium acetate. Figure 6 shows a CD measurement with fitted parameters 19% α -helix and 43% β -sheet and turn. A temperature melt was performed to determine the thermal

stability of NBD1-R (Figure 6, inset). Denaturation at 50% of NBD1-R occurred at $\sim 60^{\circ}\text{C}$.

DISCUSSION

The NBD1-R domain of human CFTR was expressed in bacteria as a single protein, purified by metal affinity chromatography under denaturing conditions, and renatured by rapid dilution at pH 5. It was necessary to evaluate multiple strategies for expression and renaturation in order to generate substantial quantities of protein that remained soluble, that bound nucleotides with high affinity, and, as demonstrated in a recent study (26), that was phosphorylated by PKA at essentially the same sites as those phosphorylated in vivo in full-length CFTR. Although renaturation procedures involving in situ reduction of denaturant concentration on the column and dialysis have been used for various soluble proteins (33), including the NBD1 and R domains of CFTR (13, 15, 17, 20), only rapid dilution into an acidic solution was successful for the NBD1-R protein. The presence of poly(ethylene glycol) or L-arginine, maneuvers that have facilitated folding NBD1-like proteins (15, 17), did not promote folding of NBD1-R. The folded NBD1-R protein remained soluble and stable in solution for months, bound TNP-ATP with high affinity, and had significant secondary structure. An interesting unexpected finding (discussed further below) was that nucleotide binding to NBD1 inhibited PKA-mediated phosphorylation of the contiguous R domain.

Secondary structure analysis of NBD1-R by circular dichroism showed $\sim 19\%$ α -helix and 43% β -sheet and turn, with no significant differences after phosphorylation. Previous studies showed 10–12% α -helix and 67–73% β -sheet and turn for NBD1 protein (12) and NBD1 isolated after cleavage of an expressed GST-NBD1 fusion protein (13). Values of 40% α -helix and 37% β -sheet and turn were found for an NBD1-MBP fusion protein (14), and 28% α -helix and 44% β -sheet and turn were reported for a His₆-tagged NBD1 protein (17). For comparison, CD analysis of a 67-mer peptide corresponding to the region of the putative ATP binding domain in NBD1 gave $<10\%$ α -helix and $\sim 80\%$ β -sheet and turn. A single study on R domain protein reported an $\sim 10\%$ α -helical content and $\sim 40\%$ β -sheet and turn (20). After phosphorylation, the α -helical content of the R domain peptide was reduced to $\sim 5\%$, suggesting a conformational change. The results here show a majority of β -sheet and turn, in general agreement with averaged values reported above for NBD1 and R domains in isolation.

The NBD1-R protein bound TNP-ATP with high affinity similar to that found in measurements on the bacterially expressed NBD1 domain alone (12) and various NBD1 fusion proteins (13, 15, 17). The high-affinity binding of TNP-ATP to its site on NBD1 arises from the ATP affinity in synergy with hydrophobic interactions of the TNP moiety. Half-maximal displacement of TNP-ATP from NBD1-R occurred at $\sim 3.2 \text{ mM}$ ATP and at ~ 4.2 and 4.6 mM for the nonhydrolyzable ATP analogues AMP-PNP and AMP-PCP, respectively. The millimolar concentration for ATP binding has been proposed as evidence that cytosolic concentrations of ATP are important for the activation of CFTR in vivo (12, 35). The TNP-ATP molar site stoichiometry was determined to be approximately 1:1, suggesting that all NBD1-R molecules are present in a similarly folded state.

TNP-ATP binding to NBD1-R was not affected by phosphorylation of the R domain, nor was there a difference in affinity for wild-type vs the Δ F508 forms of NBD1-R. These results suggest that phosphorylation of the R domain does not produce a conformational change that would result in physical blockade or altered affinity of the nucleotide binding site on NBD1. The absence of an effect of the Δ F508 mutation is consistent with previous studies showing similar thermodynamic stability and nucleotide binding affinity for the wild-type vs Δ F508 isolated NBD1 domain (15). The NBD1 domain contains the Walker A and B consensus sequences found in related nucleotide binding proteins (36) that are thought to be involved in interaction with the adenine and phosphate in ATP. From our data and the finding that the 67-mer peptide containing the Walker motifs bound TNP-ATP with high affinity (10), it is proposed that only a small region in NBD1 is involved in nucleotide binding and that the integrity of this region may be relatively insensitive to interactions not very near the binding site.

A principal finding here was that binding of ATP analogs to the NBD1 domain reduced PKA-mediated phosphorylation of the R domain. At 0.25 mM concentration, the nonhydrolyzable analogues AMP-PCP and AMP-PNP inhibited 32 P incorporation into NBD1-R by >75%; 0.25 μ M TNP-ATP inhibited 32 P incorporation by >50%. These findings are consistent with the relative binding affinities of these compounds with TNP-ATP showing >50% inhibition at 500–1000-fold lower concentration than that used for the nonhydrolyzable analogues. Importantly, these compounds did not affect PKA-mediated phosphorylation of two control proteins: Kemptide, a peptide substrate containing a single PKA consensus site, and a GST-R domain fusion protein, which contains the complete CFTR R domain. These findings suggest a significant interaction between the NBD1 and R domains during and/or after nucleotide binding that influences PKA phosphorylation of the R domain. These results are consistent with studies of CFTR Cl^- channel activation that suggested indirectly that the activities of the NBDs and R domain are linked (37, 38). The precise mechanism by which nucleotide binding to the NBD1 domain affects the efficiency of R domain phosphorylation is not defined by the studies here, but is likely to involve a protein conformational change that alters R domain conformation and/or its accessibility to PKA and ATP.

The site specificity of R domain phosphorylation was investigated following phosphopeptide purification and separation. In full-length CFTR, the *in vivo* phosphorylated residues are serines 660, 700, 737, 813, 768, and 795 (5, 22, 39). Recently, eight phosphorylated serine residues, including the six sites in full-length CFTR as well as serines 422 and 712, were identified in PKA-phosphorylated NBD1-R (26). A major peak corresponding to the serine 737-containing phosphopeptide was seen here in all samples, as well as peaks corresponding to phosphopeptides containing serines 660, 712, 795, and 813. This concurs with the finding that serine 737 is the first residue phosphorylated by PKA in an R domain (amino acids 620–830) recombinant protein (34). The absence of peaks corresponding to phosphopeptides containing serines 422, 700, and 768 may be due to the reaction conditions which were designed to give incomplete phosphorylation or they were below the detectable limits of the HPLC based assay. Therefore, multiple serines

were phosphorylated under the experimental conditions, and the nucleotides that inhibited R domain phosphorylation did not grossly affect the phosphorylation pattern.

Although the effects of nucleotides on R domain phosphorylation were quite substantial in measurements on the isolated NBD1-R domain protein, the potential implications of these findings to CFTR function *in vivo* should be made with caution. The influence of nucleotide binding on phosphorylation, taken together with the lack of effect of phosphorylation on nucleotide binding, raises the possibility of a causal relationship that might apply *in vivo*. Previous studies of Cl^- channel function in mutated CFTRs with partial R domain deletion and NBD2 mutations are consistent with an interaction between the NBD2 and R domains (38). The nonhydrolyzable nucleotide analogues AMP-PNP and pyrophosphate have been shown to lock CFTR into an open state, possibly by blocking ATP access to its site on NBD2 (37, 40). However, it is difficult to compare the present results with functional studies on full-length CFTR because of the multiple complex interactions possible in the whole protein. In particular, the functional studies cannot easily examine the possibility that NBD1 is involved in interaction with nucleotides before or after phosphorylation. The data on NBD1-R reported here suggest a role for NBD1 in interaction with nucleotides prior to channel opening, possibly in regulating the access of PKA to phosphorylation sites on the R domain.

REFERENCES

1. Frizzell, R. A. (1995) *Am. J. Respir. Crit. Care Med.* 151, S54–58.
2. Riordan, J. R. (1993) *Annu. Rev. Physiol.* 55, 609–630.
3. Riordan, J. R., Rommens, J. M., Bat-sheva, K., Alon, N., Rozmahel, R., Grzelcazk, A., Zielenski, J., Lok, S., Plavsic, N., Chou, J.-L., Drumm, M. L., Iannuzzi, M. C., Collins, F. S., and Tsui, L.-C. (1989) *Science* 245, 1066–1073.
4. Tabcharani, J. A., Chang, X.-B., Riordan, J. R., and Hanrahan, J. W. (1991) *Nature* 352, 628–631.
5. Cheng, S. H., Rich, D. P., Marshall, J., Welsh, M. J., and Smith, A. E. (1991) *Cell* 66, 1027–1036.
6. Anderson, M. P., Berger, H. A., Rich, D. P., Gregory, R. J., Smith, A. E., and Welsh, M. J. (1991) *Cell* 67, 775–784.
7. Carson, M. R., Travis, S. M., and Welsh, M. J. (1995) *J. Biol. Chem.* 270, 1711–1717.
8. Gunderson, K. L., and Kopito, R. R. (1995) *Cell* 82, 231–239.
9. Ostedgaard, L. S., Rich, D. P., DeBerg, L. G., and Welsh, M. J. (1997) *Biochemistry* 36, 1287–1294.
10. Thomas, P. J., Shenbagamurthi, P., Ysern, X., and Pedersen, P. L. (1991) *Science* 251, 555–557.
11. Arispe, N., Rojas, E., Hartman, J., Sorscher, E. J., and Pollard, H. B. (1992) *Proc. Natl. Acad. Sci. U.S.A.* 89, 1539–1543.
12. Logan, J., Hiestand, D., Daram, P., Huang, Z., Muccio, D. D., Hartman, J., Haley, B., Cook, W. J., and Sorscher, E. J. (1994) *J. Clin. Invest.* 94, 228–236.
13. Hartman, J., Huang, Z., Rado, T. A., Peng, S., Jilling, T., Muccio, D. D., and Sorscher, E. J. (1992) *J. Biol. Chem.* 267, 6455–6458.
14. Ko, Y. H., Thomas, P. J., Delannoy, M. R., and Pedersen, P. L. (1993) *J. Biol. Chem.* 268, 24330–24338.
15. Qu, B. H., and Thomas, P. J. (1996) *J. Biol. Chem.* 271, 7261–7264.
16. Thomas, P. J., and Pedersen, P. L. (1993) *J. Bioeng. Biomembr.* 25, 11–19.
17. Yike, I., Ye, J., Zhang, Y., Manavalan, P., Gerken, T. A., and Dearborn, D. G. (1996) *Protein Sci.* 5, 89–97.
18. Ko, Y. H., and Pedersen, P. L. (1995) *J. Biol. Chem.* 270, 22093–22096.

19. Dulhanty, A. M., Chang, X. B., and Riordan, J. R. (1995) *Biochem. Biophys. Res. Commun.* 206, 207–214.
20. Dulhanty, A. M., and Riordan, J. R. (1994) *Biochemistry* 33, 4072–4079.
21. Picciotto, M. R., Cohn, J. A., Bertuzzi, G., Greengard, P., and Nairn, A. C. (1992) *J. Biol. Chem.* 267, 12742–12752.
22. Seibert, F. S., Tabcharani, J. A., Chang, X.-B., Dulhanty, A. M., Matthews, C., Hanrahan, J. W., and Riordan, J. R. (1995) *J. Biol. Chem.* 270, 2158–2162.
23. Gruis, D., Riley, C., and Price, E. (1996) *Pediat. Pulmonol. Suppl.* 13, 222.
24. Pitterle, D. M., and Price, E. M. (1992) *Pediat. Pulmonol. Suppl.* 8, 262.
25. Yike, I., Zhang, Y., Ye, J., and Dearborn, D. G. (1996) *Protein Expression Purif.* 7, 45–50.
26. Townsend, R. R., Lipniunas, P. H., Tulk, B. M., and Verkman, A. S. (1996) *Protein Sci.* 5, 1865–1873.
27. Neville, D. C. A., Rozanas, C. R., Price, E. M., Gruis, D. B., Verkman, A. S., and Townsend, R. R. (1997) *Protein Sci.* 6, 2436–2445.
28. Chang, C. T., Wu, C.-S. C., and Yang, J. T. (1978) *Anal. Biochem.* 91, 13–31.
29. Buchner, J., Pastan, I., and Brinkmann, U. (1992) *Anal. Biochem.* 205, 263–270.
30. Buchner, J., and Rudolph, R. (1991) *Biotechnology* 9, 157–162.
31. Cleland, J. L. (1993) in *Biotechnology*, (Stephanopoulos, G., Ed.) Vol. 3, pp 527–555, VCH Publishers, New York.
32. Light, A. (1985) *BioTechniques* 3, 298–306.
33. Marston, F. A. (1986) *Biochem. J.* 240, 1–12.
34. Borchardt, R., Kole, J., and Cohn, J. (1996) *Pediat. Pulmonol. Suppl.* 13, 212.
35. Quinton, P. M., and Reddy, M. M. (1992) *Nature* 360, 79–81.
36. Walker, J. E., Saraste, M., Runswick, M. J., and Gay, N. J. (1982) *EMBO J.* 1, 945–981.
37. Hwang, T. C., Nagel, G., Nairn, A. C., and Gadsby, D. C. (1994) *Proc. Natl. Acad. Sci. U.S.A.* 91, 4698–4702.
38. Rich, D. P., Gregory, R. J., Anderson, M. P., Manavalan, P., Smith, A. E., and Welsh, M. J. (1991) *Science* 253, 205–207.
39. Chang, X. B., Tabcharani, J. A., Hou, Y. X., Jensen, T. J., Kartner, N., Alon, N., Hanrahan, J. W., and Riordan, J. R. (1993) *J. Biol. Chem.* 268, 11304–11311.
40. Carson, M. R., Winter, M. C., Travis, S. M., and Welsh, M. J. (1995) *J. Biol. Chem.* 270, 20466–20472.

BI972021K